Hydrodynamic electron flow in high-mobility wires

M. J. M. de Jong* and L. W. Molenkamp†
Philips Research Laboratories, 5656 AA Eindhoven, The Netherlands
(Submitted October 24, 1994 — cond-mat/9411067)

arXiv:cond-mat/9411067v1 17 Nov 1994

Abstract

Hydrodynamic electron flow is experimentally observed in the differential resistance of electrostatically defined wires in the two-dimensional electron gas in (Al,Ga)As heterostructures. In these experiments current heating is used to induce a controlled increase in the number of electron-electron collisions in the wire. The interplay between the partly diffusive wire-boundary scattering and the electron-electron scattering leads first to an increase and then to a decrease of the resistance of the wire with increasing current. These effects are the electronic analog of Knudsen and Poiseuille flow in gas transport, respectively.

The electron flow is studied theoretically through a Boltzmann transport equation, which includes impurity, electron-electron, and boundary scattering. A solution is obtained for arbitrary scattering parameters. By calculation of flow profiles inside the wire it is demonstrated how normal flow evolves into Poiseuille flow. The boundary-scattering parameters for the gate-defined wires can be deduced from the magnitude of the Knudsen effect. Good agreement between experiment and theory is obtained.

PACS numbers: 73.50.Fq, 72.10.Bg, 73.50.Lw, 73.50.Bk

Typeset using REVTEX

I. INTRODUCTION

In his 1909 paper on gas flow through a capillary, Knudsen demonstrated that the ratio between the pressure drop over the capillary and the gas-flow rate first increases and then decreases with increasing density.[1] The mechanism is that with increasing density of gas particles, the number of interparticle collisions increases. At low densities (what is now known as the Knudsen transport regime) the gas particles move almost independently, so that the flow is mainly carried by particles with a large velocity parallel to the wire axis. These particles travel long distances before colliding with the wall. An occasional interparticle collision, although not resistive by itself because of momentum conservation, drives the parallel-moving particles towards the wall and shortens their trajectories between subsequent collisions with the wall. Therefore, in this regime, an enhancement of the interparticle collision-rate leads to increasing dissipation of forward particle momentum at the capillary walls. At higher densities, however, many interparticle collisions between subsequent particle-wall collisions occur, resulting in a random-walk behavior. As a consequence a laminar (Poiseuille) flow evolves, in which the effective particle-wall interaction is decreased.

Because of the analogy between classical diffusive transport of electrons and gas particles, one anticipates that a similar transition between Knudsen and Poiseuille flow may occur in electron transport. In this case electron-electron (e-e) scattering events are the analogue of collisions between gas particles.[2] Electron-electron scattering[3] has no influence on the electrical resistivity of bulk materials, because it conserves the total momentum of the electron distribution. Effects of e-e scattering in the classical transport regime can only be expected in the resistivity of films and wires of high purity and small dimensions,[4] where conditions similar to those leading to hydrodynamic gas flow can be realized. Typically, the sample width W should be smaller than or comparable to the impurity mean free path l_b of the bulk material. These two lengths should be compared to l_{ee}, the average length an electron covers between two subsequent e-e scattering events. When $l_{ee} > W$ one expects an increase of the resistivity with increasing e-e scattering rate, which is the electronic Knudsen effect. In contrast, when $l_{ee} < W$ the resistivity should decrease with increasing e-e scattering rate, due to electronic Poiseuille flow. The latter effect has been predicted by Gurzhi in 1963[5] and is now known as the Gurzhi effect. Experimentally, it proved difficult to obtain reliable data on these effects, because dissipation mechanisms not present in gas flow usually prevent the occurrence of electronic Knudsen and Gurzhi flow regimes: First of all, electrons in a metal are scattered by impurities. Moreover, since the e-e scattering rate is usually varied by changing the lattice temperature of the sample, the induced effects are overwhelmed by electron-phonon interactions. Furthermore, an increase in temperature also enhances the *umklapp* electron-electron scattering rate, which adds to the bulk resistivity. Finally, deviations from an ideal spherical Fermi surface may hinder interpretation of experimental data.

Due to these complications, only a few experimental indications of e-e scattering effects have been found.[4] Most experiments use potassium, as an exemplary simple metal, which to a good approximation has a spherical Fermi surface.[6] However, the observed changes in the resistivity as a function of lattice temperature are limited to about 0.01% of the total resistivity, because of the small l_b and the onset of electron-phonon scattering. Yu *et al.*[7] have reported a negative temperature derivative of the resistivity ($d\rho/dT$) of potassium wires at

temperatures around and below 1 K. However, an interpretation in terms of the Gurzhi effect was disputed,[4] since at these temperatures $l_{ee} > W$. In later publications of the same group, it was shown that the negative $d\rho/dT$ can be attributed to metallurgical imperfections,[8] and also Kondo-like effects in the resistivity were reported.[9] Observations of a positive $d\rho/dT$ in wider wires[8] were interpreted by Movshovitz and Wiser[10] as a Knudsen-like behavior due to the combination of e-e and electron-phonon collisions. A similar mechanism was proposed to explain an anomalously strong, positive $d\rho/dT$ in very thin potassium films.[11,12] However, until now there has been no observation of electronic Poiseuille flow, nor has there been an observation of a 'Knudsen maximum' in the resistance[2] at the crossover between Knudsen and Gurzhi flow regimes.

In this paper, we present an experimental and theoretical study of Knudsen and Gurzhi transport phenomena in two-dimensional wires. The wires used for the experiments are defined electrostatically in the two-dimensional electron gas (2DEG) of (Al,Ga)As heterostructures.[13] Using these devices to study hydrodynamic electron-flow offers several advantages: First, due to the high purity of the material and the resolution of electron-beam lithography one can easily reach the condition $l_b > W$. Second, *umklapp* electron-electron scattering is absent, because of the low electron density and the perfectly circular Fermi surface. Third, the electron-acoustic phonon coupling is weak in the (Al,Ga)As-2DEG system. This makes it possible to investigate the influence of e-e scattering *not* by changing the temperature T of the full sample, but by selectively changing the temperature T_e of the electrons inside the wire by passing a dc current I through the device. Previously, this current-heating technique has proven very useful for the study of thermoelectric phenomena in nanostructures.[14,15] The wires studied here are equipped with opposing pairs of quantum point-contacts in their boundaries. Since the thermopower of the point contacts is quantized,[15] we can determine the electron temperature T_e in the wire, as a function of I, from a thermovoltage measurement.[16] The ability to modify selectively the e-e scattering rate allows a clear and unambiguous demonstration of hydrodynamic effects on the resistance of the wire.

We measure in the experiments the differential resistance dV/dI versus I.[17] In the resistance curves we can distinguish three regimes: 1) Starting from $I = 0$ we observe an increase in dV/dI with increasing I. This is attributed to the Knudsen effect. We find resistance changes as large as 10% of the total resistance. 2) Then there is a range where dV/dI decreases with increasing I, which we identify as the Gurzhi effect. In this range, we see relative resistance changes up to 20%. 3) Upon increasing I we come into a regime where dV/dI increases again. Here, the heating due to the applied current also affects the lattice temperature, so that the resistance increase can be attributed to enhanced electron-phonon scattering. At the crossover between regime 1) and 2) the Knudsen maximum is reached. The minimum in the resistance between regime 2) and 3) was the actual subject of one of Gurzhi's first papers.[5]

In order to understand our experimental results, we have developed a theory based on the Boltzmann transport equation, which yields quantitative agreement with the experiments. In the first half of this century the Boltzmann approach has been applied to study size effects on the resistance of small conductors. The thin film case has been addressed by Fuchs[18] and the case of a thin wire by Dingle.[19] A particularly insightful method to solve the Boltzmann equation is due to Chambers,[20] who has expressed the solution in terms of the effective mean

free path the electron covers between either bulk-impurity or boundary collisions. These treatments consider partially diffusive boundary scattering, in which part of the electrons colliding with the boundaries is specularly reflected and the remainder is diffusely scattered. The boundary scattering is modeled by a constant specularity coefficient. In a more realistic treatment by Soffer[21] the wave nature of the electrons has been taken into account and results in a specularity coefficient which depends on the angle of incidence. In Ref. 22 it is shown that inclusion of the angle-dependent specularity coefficient in a calculation of the resistivity of thin wires gives a more satisfactory agreement with experiments than Dingle's original theory.

The inclusion of e-e scattering in the Boltzmann approach to the resistivity of wires is not trivial and has been limited to a certain parameter range in most treatments. In the pioneering work by Gurzhi,[5] the situation $l_{ee} \ll l_b, W$ is considered. It is shown that under these conditions the Boltzmann equation can be mapped on a Navier-Stokes type of equation. The opposite Knudsen regime $l_{ee} \gg l_b, W$ has been treated by Movshovitz and Wiser,[10,11] who use the Chambers method to calculate effective mean free paths with the approximation that at most one e-e scattering event in each electron trajectory is taken into account. In Ref. 23 Gurzhi and coworkers provide an alternative approach for this regime, by solving the Boltzmann equation perturbatively. This also allows including specific features of the e-e scattering, such as the distinction between isotropic and small-angle scattering. We know of only two approaches that describe the resistivity of wires from the Knudsen up to the Gurzhi regime. The first is due to Black,[24] who employs a Monte Carlo technique to calculate effective mean free paths in a wire. Although the numerical results are not so accurate because of the limited computer power available at the time, the Knudsen maximum in the resistivity is found. The results show similar behavior for isotropic and small-angle e-e scattering. The second approach is due to De Gennaro and Rettori.[25] They start from the Boltzmann equation and include e-e scattering by a scattering term due to Callaway[26] in which the electrons are relaxed towards a distribution with a net drift velocity. As pointed out by Gurzhi *et al.*,[23] the final results of Ref. 25 are incorrect, because the spatial variation of the drift velocity is neglected.

Our theoretical description starts from a kinetic equation similar to that of Ref. 25. We have obtained a self-consistent solution of the relevant Boltzmann equation. This is the first theory which provides an analytical expression for the Boltzmann distribution function for *any* set of l_{ee}, l_b, W. It will prove insightful to express the Boltzmann distribution function in terms of an effective mean free path. For the regime $l_{ee} \gg l_b, W$ our solution is equivalent to the results of Movshovitz and Wiser, so that we have provided a formal basis for their method of including e-e scattering events in the electron trajectories. Our approach is indeed able to describe the transition from Knudsen to Poiseuille flow. The transition can be illustrated by the evolution of the electron-flow profiles along the wire.

In the three-dimensional case, which has been addressed in most previous treatments, the e-e scattering rate of electrons in a thermal slice around the Fermi surface is proportional to T^2, as follows from the well-known phase space argument.[2] For a 2DEG, instead, the e-e scattering rate is proportional to $T^2 \ln T$.[27,28] In a study by Laikhtman[29] of relaxation of injected electrons into a zero-temperature 2DEG it is found that small-angle scattering is important. Features of e-e scattering in a 2DEG are also discussed by Gurzhi and coworkers.[30] The e-e scattering term which we use is first proposed by Callaway[26] and is

not of a microscopic origin, but takes the main feature of e-e scattering, conservation of momentum, into account. As we will show, an attractive feature of this simplified scattering term is that it allows an exact (numerical) solution of the Boltzmann equation.

We have compared experiment with theory through a three step procedure: First, using the results of the point-contact thermometry we find T_e versus I. Then, using a formula due to Giuliani and Quinn[28] we calculate l_{ee} as a function of T_e. Finally, we determine the wire resistivity for the given l_{ee} from our Boltzmann approach. This has yielded quite a satisfactory agreement for both the Knudsen and the Gurzhi regime. The regime 3) in which phonon scattering due to the heating of the lattice increases the resistivity is outside the range of our theory. From the magnitude of the Knudsen effect we obtain information on the boundary-scattering parameters of the gate-defined wires.

A brief account of this work with an emphasis on the experiments has already been published.[31] Here, we present a more extensive discussion. Particular attention is paid to the derivation of the theoretical model and how its results can be compared with the experiments. The outline of this paper is as follows: In Sec. II the experiments are presented. Sec. III describes the theoretical model formulated in terms of a Boltzmann equation. The method of solution and the theoretical results including flow profiles are studied in Sec. IV. Sec. V discusses the comparison between theory and experiment. Finally, we conclude in Sec. VI. Appendix A and B detail some technical parts of the calculation.

II. EXPERIMENTAL OBSERVATION OF KNUDSEN AND GURZHI TRANSPORT REGIMES

Our devices are fabricated from two different (Al,Ga)As heterostructures containing a high-mobility 2DEG, grown at Philips Research Laboratories, Redhill, Surrey, UK. The wires used in the experiments are created by electrostatic confinement of the 2DEG using a split gate technique. On top of the heterostructures, which are mesa-etched in the shape of a Hall bar, a pattern of TiAu gates is defined using electron-beam lithography. The lay-out of the TiAu gates is given schematically in the inset of Fig. 1. The wires have a lithographic width $W_{\rm lith} \simeq 4.0\,\mu$m (note that due to electrostatic depletion the width W of the wires in the 2DEG is somewhat smaller), and a length L that varies between 20 and 120 μm. A quantum point-contact[13] is incorporated in each wire boundary. We report here on three different types of samples, whose particulars as to L, W, electron density n and mean free path l_b are summarized in Table I. For transport measurements, the samples are kept in a cryostat at temperatures of 1.5 K and above, and at zero magnetic field. For reasons of sensitivity, we measure the differential resistance of point contacts and wires with standard low-frequency lock-in techniques, using a 100 μV ac voltage. All measurements are performed in a four-terminal geometry.

In order to adjust the electron temperature in the wires, a dc heating current $I \equiv I_{15}$ (typically an order of magnitude larger than the ac measuring current) is passed through the wire using Ohmic contacts 1 and 5. Because of power dissipation, the average kinetic energy of the electrons in the wire increases. Due to frequent e-e scattering events, the electron distribution-function in the wire thermalizes rapidly to a heated Fermi function at a temperature T_e, above the lattice temperature T. This increased electron temperature can be measured using the quantum-point contacts in the wire boundaries: since the electrons in

the regions outside the wire remain at the same temperature as the lattice, a thermovoltage builds up across both point contacts AB and CD, which can be measured as a transverse voltage $V_{\rm trans} \equiv V_6 - V_3$. Note that $V_{\rm trans}$ does not contain a contribution from the voltage drop along the wire, since point contacts AB and CD face each other. We thus have

$$V_{\rm trans} \equiv V_6 - V_3 = (S_{\rm AB} - S_{\rm CD})(T_e - T)\,, \tag{1}$$

where $S_{\rm AB(CD)}$ denotes the thermopower of point contact AB(CD).

Like the electrical conductance, the thermopower S of a quantum point-contact exhibits a pronounced quantum size-effect:[32,15] while the electrical conductance of the point contact varies stepwise with the voltage on the split-gates, the thermopower oscillates. The external gate voltage controls the number of one-dimensional subbands present below the Fermi energy in the point contact. When the Fermi energy inside the point contact falls in between two subbands, the conductance is quantized, and the thermopower $S \simeq 0$. However, when the Fermi energy inside the point contact exactly coincides with the bottom of the N-th subband, the conductance is in between the N-th and the $(N-1)$-th plateau, and the thermopower attains a maximum value, which for a step-function transmission probability of the point contact, is given by[32]

$$S = -\frac{k_B}{e}\frac{\ln 2}{N - \frac{1}{2}}\,, \tag{2}$$

if $N > 1$. The quantum oscillations in the thermopower of a quantum point-contact were predicted by Streda,[32] and an experimental demonstration of the effect has been reported elsewhere.[15] Here, we utilize the effect to measure the electron temperature in the wire: we adjust point contact CD on a conductance plateau, thus setting $S_{\rm CD} \simeq 0$, and adjust point contact AB for maximum thermopower [$G_{\rm AB} = 1.5 \times (2e^2/h)$, where $S_{\rm AB} \simeq -40\ \mu$V/K]. The result of such a measurement of $V_{\rm trans}$ as a function of dc heating current I, obtained for a wire of type I, is shown in Fig. 1. For the longer wires a very similar behavior is found. In general, we find that for $|I| \lesssim 20\,\mu$A, and a lattice temperature $T \lesssim 2$ K, the electron temperature T_e in the wire is approximately given by

$$T_e = T + (I/W)^2 \sigma^{-1}\, C\,, \tag{3}$$

where σ is the conductivity of the wire. The constant $C \simeq 0.05$ m^{2}K/W. Evidently, such a quadratic dependence of T_e on I is exactly what one expects to a first approximation for Joule dissipation. For $|I| \gtrsim 20\,\mu$A, the situation is more complicated since at these current levels also the lattice temperature starts to increase.

The hydrodynamic electron-flow effects that are the subject of this article are observed in the differential resistance $dV/dI \equiv dV_{24}/dI_{15}$ of our wires, as a function of dc heating current I.[17] Experimental results obtained for wires I, II, and III for a series of lattice temperatures are given in Figs. 2 and 3. Also shown are theoretical results that will be discussed in Sec. V. A strongly non-monotonic behavior of dV/dI is evident for all traces. This non-monotonic behavior in the differential resistance is the focus of this paper and we will show that it results from electronic Knudsen and Poiseuille flow.

A first remark we should make here is that in the high-mobility 2DEG quantum corrections to the resistance such as weak localization are not measurable at the temperatures

involved. This means that the non-monotonic behavior must result from classical effects. Note further that for the low lattice-temperature results of Figs. 2 and 3 all three resistance regimes indicated in the Introduction can be observed: 1) Increasing dV/dI due to Knudsen flow, 2) decreasing dV/dI in the Gurzhi regime, and 3) a quasi-parabolically increasing dV/dI due to lattice heating. Only in the last regime, we find from a nearby thermometer that the lattice temperature of the sample increases, implying that the quasi-quadratic behavior 3) is due to Joule heating of the lattice in combination with the linear increase of electron-phonon scattering.[33] Wire I (cf. Fig. 2) exhibits a smaller Knudsen effect (and only at the lowest lattice temperature studied) than wires II and III. As we will demonstrate below, this results from the smaller ratio l_b/W in wire I, compared to wires II and III. If the lattice temperature T is increased we observe in Fig. 2 two distinct effects. First, the $I = 0$ resistance increases. This is due to the decrease of l_b by additional electron-phonon scattering. Second, the hydrodynamic effects on the resistance disappear, the Knudsen effect at lower T than the Gurzhi effect. This is caused by the decrease of l_{ee} at $I = 0$ (where $T_e = T$) with increasing lattice temperature. Another point to notice in Fig. 3 is that the magnitude of the initial increase of dV/dI (the Knudsen effect) is twice as large for wire III as for wire II. This shows that the effect scales with the length of the wire and does not stem from e.g. the wire entrances.

To see whether the hydrodynamic electron-flow phenomena mentioned in Sec. I can indeed be responsible for the anomalous behavior of dV/dI, it is instructive to estimate for wire I the e-e scattering mean free path l_{ee} for a current $I = 15\,\mu$A, i.e. in the regime of decreasing dV/dI. According to Eq. (3), $I = 15\,\mu$A corresponds to an electron temperature $T_e \approx 16\,$K (for a lattice temperature $T = 1.5\,$K). We have $l_{ee} = v_F\tau_{ee}$, where v_F is the Fermi velocity, and τ_{ee} the e-e scattering time, given by[28,34,35]

$$\frac{1}{\tau_{ee}} = \frac{E_F}{h}\left(\frac{k_BT_e}{E_F}\right)^2\left[\ln\left(\frac{E_F}{k_BT_e}\right) + \ln\left(\frac{2q}{k_F}\right) + 1\right] . \tag{4}$$

Here $q = me^2/2\pi\varepsilon_r\varepsilon_0\hbar^2$ is the Thomas-Fermi screening wavevector. We find $l_{ee} \approx 0.8\,\mu$m, which is much smaller than W. In this limit, the electrons undergo a random-motion due to frequent e-e scattering events, and we assign, at this stage tentatively, the decrease in dV/dI to the Gurzhi effect. For currents below $8\,\mu$A, dV/dI is positive. As $l_{ee} \approx 5\,\mu\text{m} \approx W$ for $I = 8\,\mu$A and $T = 1.5\,$K, the positive dV/dI occurs in the right current range for the electronic Knudsen effect. In the following Sections we will formulate our calculations that substantiate the assignment of the anomalous behavior of dV/dI to hydrodynamic electron flow.

III. BOLTZMANN EQUATION

We study the electron flow inside a two-dimensional wire of width W in response to a constant electric field $\mathbf{E}$, applied in the x-direction, parallel to the wire. The 2DEG has an ideal circular Fermi surface. We look for a time-independent distribution function $f(\mathbf{r}, \mathbf{k})$ for electrons at position $\mathbf{r} = (x, y)$ and with wavevector $\mathbf{k} = k(\cos\varphi, \sin\varphi)$ (see inset of Fig. 1), which obeys the stationary Boltzmann transport equation

$$e\mathbf{E}\cdot\frac{\partial f(\mathbf{r},\mathbf{k})}{\hbar\partial\mathbf{k}}+\mathbf{v}\cdot\frac{\partial f(\mathbf{r},\mathbf{k})}{\partial\mathbf{r}}=\left.\frac{\partial f(\mathbf{r},\mathbf{k})}{\partial t}\right|_{\rm scatt}\,, \tag{5}$$

where the r. h. s. is the scattering term, taking into account both electron-impurity and e-e scattering. Application of the electric field leads to a disturbance of the distribution function from its equilibrium Fermi-Dirac distribution $f_0(\varepsilon)=1/\{1+\exp[(\varepsilon-E_F)/kT_e]\}$ for energy $\varepsilon=\hbar^2k^2/2m=mv^2/2$ and with Fermi energy E_F. At not too high fields, the non-equilibrium part of the electron distribution function is only in a small shell around the Fermi surface. Therefore, and using the translational invariance along the x-axis, we write the distribution function as

$$f(\mathbf{r},\mathbf{k})=f_0(\varepsilon)+\left(-\frac{\partial f_0}{\partial\varepsilon}\right)\chi(y,\varphi)\,. \tag{6}$$

Substitution of Eq. (6) into Eq. (5) yields in linear response

$$-e\mathbf{E}\cdot\mathbf{v}+\mathbf{v}\cdot\hat{\mathbf{y}}\frac{\partial\chi(y,\varphi)}{\partial y}=\left.\frac{\partial\chi(y,\varphi)}{\partial t}\right|_{\rm scatt}\,, \tag{7}$$

where $\hat{\mathbf{y}}$ is the unit vector in the y-direction. We neglect the energy dependence of the velocity in the thermal region around the Fermi energy, so that $\mathbf{v}=v_F(\cos\varphi,\sin\varphi)$.

Once the distribution function has been evaluated, the current density can be calculated according to

$$\begin{aligned}\mathbf{j}(y)&=2\sum_{\mathbf{k}}f(\mathbf{r},\mathbf{k})e\mathbf{v}\,,\\&=\int d\varepsilon\mathcal{D}(\varepsilon)\left(-\frac{\partial f_0}{\partial\varepsilon}\right)\int_0^{2\pi}\frac{d\varphi}{2\pi}\chi(y,\varphi)e\mathbf{v}\,,\\&=e\mathcal{D}v_F\int_0^{2\pi}\frac{d\varphi}{2\pi}\chi(y,\varphi)\hat{\mathbf{v}}\,,\end{aligned} \tag{8}$$

with the two-dimensional density of states $\mathcal{D}(\varepsilon)=\mathcal{D}=m/\pi\hbar^2$ (assuming a two-fold spin-degeneracy) and with unit vector $\hat{\mathbf{v}}=(\cos\varphi,\sin\varphi)$.

Let us now specify the scattering terms on the r. h. s. of Eq. (7). The scattering by bulk impurities is assumed to be elastic and isotropic. This implies for the scattering term

$$\left.\frac{\partial\chi(y,\varphi)}{\partial t}\right|_b=-\frac{\chi(y,\varphi)}{\tau_b}+\frac{1}{\tau_b}\int_0^{2\pi}\frac{d\varphi'}{2\pi}\chi(y,\varphi')\,, \tag{9}$$

where τ_b denotes the electron-impurity scattering time. Note that the second term on the r. h. s. of Eq. (9) representing the electrons scattered *into* (y,φ) is omitted in many treatments of the Boltzmann transport equation. In these cases it is *a priori* assumed that the non-equilibrium density is zero. For completeness, we maintain this term here and show explicitly that it equals zero for our complete Boltzmann equation in Appendix A. For the e-e scattering term we follow Refs. 25,26 (the Callaway ansatz)

$$\left.\frac{\partial\chi(y,\varphi)}{\partial t}\right|_{ee} = -\frac{\chi(y,\varphi)}{\tau_{ee}} + \frac{1}{\tau_{ee}}\int_0^{2\pi}\frac{d\varphi'}{2\pi}\chi(y,\varphi') + \frac{m\mathbf{v}\cdot\mathbf{v}_{\rm drift}(y)}{\tau_{ee}}\,, \tag{10}$$

with τ_{ee} the e-e scattering time and $\mathbf{v}_{\rm drift}$ the net drift velocity. The e-e scattering term (10) implies that the electrons are relaxed towards a shifted distribution function $f(\mathbf{r},\mathbf{k}) = f_0(\varepsilon - m\mathbf{v}\cdot\mathbf{v}_{\rm drift})$. The second term on the r. h. s. of Eq. (10) again ensures the conservation of particle density. The drift velocity is related to the current density (8) according to $\mathbf{j}(y) = ne\mathbf{v}_{\rm drift}$ with the electron density $n = \mathcal{D}E_F$, so that Eq. (10) becomes

$$\left.\frac{\partial\chi(y,\varphi)}{\partial t}\right|_{ee} = -\frac{\chi(y,\varphi)}{\tau_{ee}} + \frac{1}{\tau_{ee}}\int_0^{2\pi}\frac{d\varphi'}{2\pi}\chi(y,\varphi')(1+2\hat{\mathbf{v}}'\cdot\hat{\mathbf{v}})\,. \tag{11}$$

One readily verifies that this scattering term conserves the total momentum

$$\int_0^{2\pi} d\varphi\,\left.\frac{\partial\chi(y,\varphi)}{\partial t}\right|_{ee}\hat{\mathbf{v}} = \mathbf{0}\,. \tag{12}$$

Actually, Eq. (11) is the simplest possible scattering term with this property. Since the scattering probability from direction φ to φ' is proportional to $1+2\hat{\mathbf{v}}'\cdot\hat{\mathbf{v}} = 1+2\cos(\varphi-\varphi')$, small-angle forward scattering ($\varphi - \varphi' \approx 0$) is most probable. The negative values for $\varphi-\varphi' \approx \pi$ correspond to the scattering of a non-equilibrium electron into a non-equilibrium hole in the opposite direction.[30]

For the scattering with the boundaries of the wire it is assumed that a fraction p of the incoming electrons is scattered specularly, whereas the remainder is scattered diffusely. In the original theories of size effects[18–20] the specularity coefficient p is taken to be angle independent. A microscopic model by Soffer[21] for the scattering of the incoming waves by the boundary roughness, finds that p depends on the angle of incidence

$$p(\varphi) = \exp[-(\alpha\sin\varphi)^2]\,. \tag{13}$$

This shows that electrons with grazing incidence ($\sin\varphi \to 0$) approach a unit probability of specular reflection. The parameter $\alpha = 4\pi\delta/\lambda_{\rm F}$, depends on the ratio between δ, the root-mean-square boundary-roughness, and the Fermi wavevector.

The boundary conditions for the solution of the Boltzmann equation (7) are determined by demanding particle conservation. For the $y = 0$ boundary we have

$$\chi(0,\varphi) = p(\varphi)\chi(0,2\pi-\varphi) + \int_\pi^{2\pi}\frac{d\varphi'}{\pi}[1-p(\varphi')]\chi(0,\varphi')\,, \tag{14a}$$

if $\varphi \in [0,\pi]$, and for the $y = W$ boundary

$$\chi(W,\varphi) = p(\varphi)\chi(W,2\pi-\varphi) + \int_0^{\pi} \frac{d\varphi'}{\pi}[1-p(\varphi')]\chi(W,\varphi') \,, \tag{14b}$$

if $\varphi \in [\pi, 2\pi]$. The first term on the r. h. s. represents the specularly reflected electrons, the second term the ones that are diffusely scattered.

To proceed, the non-equilibrium part of the distribution function is written as[20]

$$\chi(y,\varphi) = eE\cos\varphi\, l_{\rm eff}(y,\varphi) \,. \tag{15}$$

Here, the effective mean free path $l_{\rm eff}(y,\varphi)$ can be interpreted as the average length an electron at y in the direction φ has covered since the last boundary or impurity collision, as we show below. It is clear that a replacement of $l_{\rm eff}(y,\varphi)$ in Eq. (15) by the bulk mean free path l_b yields the well-known bulk solution of the Boltzmann equation. Let us now introduce mean free paths for bulk-impurity scattering $l_b = v_F\tau_b$, for e-e scattering $l_{ee} = v_F\tau_{ee}$, and for the combination of those two ${l^{-1}} = {l_b}^{-1} + {l_{ee}}^{-1}$. As demonstrated explicitly in Appendix A, substitution of Eq. (15) into the combined Eqs. (7), (9), and (11) gives

$$\sin\varphi\frac{\partial l_{\rm eff}(y,\varphi)}{\partial y} + \frac{l_{\rm eff}(y,\varphi)}{l} = 1 + \frac{\tilde{l}_{\rm eff}(y)}{l_{\rm ee}} \,, \tag{16}$$

$$\tilde{l}_{\rm eff}(y) = \int_0^{2\pi} \frac{d\varphi}{\pi}\cos^2\varphi\, l_{\rm eff}(y,\varphi) \,. \tag{17}$$

The integro-differential equation (16) constitutes a major simplification with respect to our starting point. This result is the basis of our further analysis in the following Section. The average effective mean free path $\tilde{l}_{\rm eff}(y)$ is directly proportional to the drift velocity

$$\mathbf{v}_{\rm drift}(y) = \frac{e\mathbf{E}}{mv_F}\tilde{l}_{\rm eff}(y) \,, \tag{18}$$

as follows from Eqs. (8), (15), and (17). The conductivity of the wire, defined according to $\mathbf{j} = \sigma\mathbf{E}$, is given by

$$\sigma = \frac{ne^2}{mv_F}\int_0^W \frac{dy}{W}\tilde{l}_{\rm eff}(y) = \frac{ne^2}{mv_F}L_{\rm eff} \,. \tag{19}$$

The overall effective mean free path $L_{\rm eff}$ is directly proportional to the conductivity and will be used instead of σ below.

IV. THEORETICAL RESULTS

As a preliminary application of Eq. (16) we briefly treat the case of transport through a bulk conductor. We thus seek a solution of the Boltzmann transport equation independent of the spatial coordinates. As a consequence of the disappearance of the y-dependence in

Eq. (16) it follows that the effective mean free path $l_{\rm eff}$ is independent of φ as well, so that [from Eq. (17)] $\tilde{l}_{\rm eff} = l_{\rm eff}$. The solution of Eq. (16) is then easily found

$$l_{\rm eff} = \frac{1}{l^{-1} - l_{ee}^{-1}} = l_b \, . \tag{20}$$

Note, that substitution into Eq. (15) produces the ordinary bulk solution of the Boltzmann equation in the absence of e-e scattering. This solution is thus shown to be *independent* of the e-e scattering rate. It clearly demonstrates, that momentum-conserving e-e scattering does not influence the bulk conductivity.

Let us now return to the wire, for which e-e scattering can have a prominent influence on the conductivity. As shown in Appendix A, it follows from a symmetry argument that $l_{\rm eff}(y,\varphi) = l_{\rm eff}(y,\pi-\varphi)$ for all φ. It is then clear from Eq. (15) that the second term on the r. h. s. of both Eqs. (14a) and (14b) vanishes. The solution of Eq. (16) in combination with the boundary conditions (14) can be written in the form of an integral equation. For clarity we first treat the case of completely diffusive boundary scattering $p = 0$. We then have for $\varphi \in [0,\pi]$

$$\begin{aligned} l_{\rm eff}(y,\varphi) = & \int_0^y \frac{dy'}{l\sin\varphi}\,\frac{y-y'}{\sin\varphi} e^{-(y-y')/l\sin\varphi} \\ & + \frac{y}{\sin\varphi} e^{-y/l\sin\varphi} \\ & + \int_0^y \frac{dy'}{l_{ee}\sin\varphi}\,\tilde{l}_{\rm eff}(y') e^{-(y-y')/l\sin\varphi} \, , \end{aligned} \tag{21a}$$

and for $\varphi \in [\pi, 2\pi]$

$$\begin{aligned} l_{\rm eff}(y,\varphi) = & \int_y^W \frac{dy'}{l|\sin\varphi|}\,\frac{y'-y}{|\sin\varphi|} e^{-(y'-y)/l|\sin\varphi|} \\ & + \frac{W-y}{|\sin\varphi|} e^{-(W-y)/l|\sin\varphi|} \\ & + \int_y^W \frac{dy'}{l_{ee}|\sin\varphi|}\,\tilde{l}_{\rm eff}(y') e^{-(y'-y)/l|\sin\varphi|} \, . \end{aligned} \tag{21b}$$

Eq. (21) elucidates the meaning of the effective mean free path $l_{\rm eff}(y,\varphi)$ as follows: Each electron arriving at y in the direction φ has covered a certain path length since the last diffusive scattering event. The first term on the r. h. s. of Eq. (21a) takes into account the length covered from the last scattering event at any y' in between 0 and y. The exponential factor gives the probability that the particle indeed reaches y without any additional scattering, whereas the distance covered is given by $(y-y')/\sin\varphi$. Note, that the scattering event at y' might have been either diffusive impurity scattering or e-e scattering. In the latter case, also the path before the scattering event must be accounted for, which is done by the last term. The second term denotes the contribution of electrons after diffusive boundary scattering. This interpretation of the solution of the Boltzmann equation is originally due

to Chambers.[20] The above derivation demonstrates that this approach is still feasible when an e-e scattering term is included in the Boltzmann equation. However, the solution itself is certainly more difficult to obtain, since Eq. (21) must be solved self-consistently with Eq. (17).

Previously, Movshovitz and Wiser have evaluated the effect of e-e scattering on the resistivity of (three-dimensional) films[11] and wires[10] by calculating effective mean free paths with at most one e-e scattering event per trajectory. This approach (most extensively described in Ref. 11) yields valid results for the Knudsen regime $l_{ee} \gg W, l_b$. We can treat this regime conveniently within our formalism by solving Eq. (21) perturbatively. Only the result of the first two terms of Eq. (21) is substituted into the third term. One can prove that this procedure is precisely equivalent to that of Ref. 11.

In Appendix B we discuss a perturbative analysis for the two-dimensional wire with diffusive boundary scattering ($p = 0$). Here, we present the main results. For the limit $l_b \gg W$ the conductivity [see Eq. (19)] in the absence of e-e scattering is given by

$$L_{\text{eff}} = \frac{2W}{\pi} \left[\ln(l_b/W) + \ln 2 + \tfrac{1}{2} - \gamma \right] , \tag{22}$$

where γ is Euler's constant (see Appendix B). In this limit the conductivity is directly proportional to the width, whereas the dependence on the mean free path is only present in the form of a logarithm. The perturbative solution allows us to calculate the first order correction to the conductivity due to e-e scattering. For the situation $l_{ee} \gg l_b \gg W$ we find

$$\Delta L_{\text{eff}} = -\frac{2W l_b}{\pi l_{ee}} . \tag{23}$$

We note that the conductivity *decreases* due to the e-e scattering. This is the Knudsen effect. It is clear from Eqs. (22) and (23) that the larger l_b/W the more prominent this effect becomes. Previous calculations for this regime has yielded $\Delta L_{\text{eff}} = -\frac{3}{4} W l_b/l_{ee}$ for a three-dimensional film of thickness W[11] and $\Delta L_{\text{eff}} \sim -(W^2/l_{ee}) \ln(l_{ee}/W)$ for a three-dimensional wire of diameter W.[23]

For the opposite limiting regime $l_b \ll W$ the influence of the boundary scattering on the conductivity becomes quite small. From the analysis in Appendix B we obtain

$$L_{\text{eff}} = l_b - \frac{4 l_b^2}{3\pi W} . \tag{24}$$

The diffusive boundary scattering yields a small negative correction to the bulk conductivity. The first order influence of e-e scattering in the regime $l_{ee} \gg W \gg l_b$ is

$$\Delta L_{\text{eff}} = \frac{4 l_b^3}{15\pi W l_{ee}} . \tag{25}$$

Apparently, in this limit e-e scattering always *increases* the conductivity, which can be understood as follows: Since e-e scattering does not influence the bulk conductivity, it can only change the small negative correction due to the boundary scattering, represented by the second term in Eq. (24). Electron-electron scattering decreases this correction, which can be interpreted as the onset of the Gurzhi effect. For comparison, we again mention

results for three dimensions: $\Delta L_{\rm eff} = \frac{6}{35}(\frac{9}{8} - \ln 2) l_b^4/W l_{ee}$ for a film (this can be calculated from the results given in Ref. 11) and $\Delta L_{\rm eff} \sim l_b^3/W l_{ee}$ for a wire.[23]

The calculation of the first order correction on the conductivity due to e-e scattering thus displays an opposite behavior in the two limiting regimes. This raises the question how $\Delta L_{\rm eff}$ crosses over from a positive value at small l_b/W to a negative value at large l_b/W. One expects that the negative correction to the conductivity appears when $l_b > W$. To substantiate this expectation, we have calculated the correction for the full regime of the ratio l_b/W. Details of this calculation are given in Appendix B. The results are presented in Fig. 4, which depicts both the conductivity in the absence of e-e scattering as well as the relative first order correction due to e-e scattering as a function of l_b/W. For the conductivity one observes a crossover from bulk-like behavior [Eq. (24)] to the logarithmic dependence of Eq. (22). The first order correction in the conductivity due to e-e scattering goes from a positive to a negative value. We find that the Knudsen effect is only present for $l_b \gtrsim 1.3W$.

The above results are valid for the regime of very low e-e scattering rate. However, in order to compare with the experiments we must also obtain solutions of Eq. (16) for the regime in which l_{ee} becomes comparable with and smaller than l_b, W. In addition, we need to incorporate the boundary condition (14) for arbitrary specularity coefficient $p(\varphi)$. By transforming Eq. (16) into an integral equation and integrating over φ we find

$$\tilde{l}_{\rm eff}(y) = \tilde{l}^{(0)}_{\rm eff}(y) + \int_0^W dy' G(y,y') \tilde{l}_{\rm eff}(y') \,, \tag{26}$$

$$\tilde{l}^{(0)}_{\rm eff}(y) = l - \frac{2l}{\pi} \int_0^{\pi/2} d\varphi \, \cos^2\varphi \times \frac{[1-p(\varphi)]\left[e^{-y/l\sin\varphi} + e^{-(W-y)/l\sin\varphi}\right]}{1-p(\varphi)e^{-W/l\sin\varphi}} \,, \tag{27}$$

$$G(y,y') = \frac{2}{\pi l_{ee}} \int_0^{\pi/2} d\varphi \, \frac{\cos^2\varphi}{\sin\varphi} \left\{ e^{-|y-y'|/l\sin\varphi} + \frac{p(\varphi)\left[e^{-(y+y')/l\sin\varphi} + e^{-(2W-y-y')/l\sin\varphi}\right]}{1-p(\varphi)e^{-W/l\sin\varphi}} \right\} . \tag{28}$$

These are the key equations which allow the evaluation of the conductivity for all values of l_{ee}, l_b, W, and p. Essentially, the $\tilde{l}^{(0)}_{\rm eff}$ term is the two-dimensional equivalent of the Fuchs solution[18] of the Boltzmann equation. The second term in Eq. (26) is a classical electron propagator-function which takes the correction due to e-e scattering into account. Note, that the perturbative approach as described in Appendix B is equivalent to the approximation $\tilde{l}_{\rm eff} = (1+G)\tilde{l}^{(0)}_{\rm eff}$. However, for larger values of l_{ee} Eq. (26) must be solved self-consistently according to $(1-G)\tilde{l}_{\rm eff} = \tilde{l}^{(0)}_{\rm eff}$. This can be achieved numerically by discretizing the y-axis, so that Eq. (26) becomes a matrix equation. This scheme allows the evaluation of the solution

$\tilde{l}_{\rm eff}$ with a precision which is only limited by the available computer power. We have used at least 400 gridpoints in our calculations to obtain sufficient precision.

In Fig. 5 the conductivity for a wire with diffusive boundary scattering ($p = 0$) is plotted against the e-e scattering length for various values of the bulk-impurity mean free path. For a wide wire ($l_b/W = 0.2$) the conductivity remains approximately constant over the full range of l_{ee}/W. The cases $l_b/W = 0.5, 1$ display a monotonous increase of $L_{\rm eff}$ with decreasing l_{ee}, the Gurzhi effect. Only for wires of width smaller than the mean free path ($l_b/W = 2, 5, 10$) can both the Knudsen *and* the Gurzhi regimes be reached: an initial decrease followed by an increase of $L_{\rm eff}$ with decreasing l_{ee} is found from the calculation. The Knudsen minimum in the conductivity is reached at $l_{ee} \simeq W$. It is clear that both the Knudsen effect and the Gurzhi effect on the conductivity become more prominent for larger ratios l_b/W. We furthermore note that the conductivity saturates to its bulk value ($L_{\rm eff} \to l_b$) when the e-e scattering rate becomes high ($l_{ee} \to 0$), which reflects the vanishing influence of the boundaries in this regime.

Let us now have a closer look at the effect of the boundary scattering. Fig. 6 displays the conductivity of a $l_b/W = 5$ wire for various angle-independent specularity coefficients p. The conductivity increases with decreasing diffusive boundary scattering. Besides this, we observe that for all $p < 1$ both the Knudsen and the Gurzhi effect are found. If the boundary scattering is fully specular ($p = 1$), $L_{\rm eff} = l_b$ regardless of the amount of e-e scattering. Essentially, the situation of specular boundary scattering is equivalent to the bulk case, in which the effects of e-e scattering are absent. It is easily checked that $\tilde{l}_{\rm eff}(y) = l_b$ solves Eq. (26) for $p = 1$. The relative conductivity change at the Knudsen maximum $\Delta L_{\rm eff}/L_{\rm eff}$ (with respect to the $l_{ee} = \infty$ value) is depicted in the inset to Fig. 6. It decreases when the boundary scattering becomes less diffuse.

As we have remarked above, the modeling of the boundary scattering by a constant specularity coefficient is only approximate. Soffer[21] has shown that a better description is given by the angle-dependent specularity coefficient of Eq. (13). Since the hydrodynamic effects in the conductivity are caused by the interplay between the e-e scattering and the boundary scattering, one may expect that the angle dependence leads to differences in the magnitude of the Knudsen and Gurzhi effects. Results comparing both models of boundary scattering are shown in Fig. 7. The parameters in both models are adjusted to yield equal conductivity in the absence of e-e scattering. It is clear from Fig. 7 that the angle-dependent scattering leads to a much larger Knudsen effect. The reason is as follows: The conductivity is mainly determined by electrons that move nearly parallel to the wire axis. These electrons hit the boundaries at grazing incidence. In the Soffer model electrons at grazing incidence experience a rather high boundary specularity. However, to have an equal conductivity for both models in the absence of e-e scattering, the boundary scattering of electrons with larger incoming angles must be more diffusive in the Soffer model. It is clear that this enhances the Knudsen effect.

So far, we have focused solely on the conductivity. More insight in the microscopic processes inside the wire can be obtained from the solution $\tilde{l}_{\rm eff}(y)$. Since it is proportional to the drift velocity according to Eq. (18), it represents the flow profile across the wire. Profiles for $l_b = 5.5W$ and $\alpha = 0.7$ and various amounts of e-e scattering are shown in Fig. 8. In the absence of e-e scattering the drift velocity is almost constant as a function of y. On increasing the e-e scattering rate, the flow profile over the full crosssection of the

wire shifts downwards due to the Knudsen effect: Occasional e-e scattering events bend the electrons moving parallel to the wire axis towards the boundaries. This effectively decreases the drift velocity and thus the conductivity. However, for smaller l_{ee} values the flow profile develops a distinct curvature. This indicates that electrons near the boundaries experience more friction due to diffusive boundary scattering than electrons in the middle of the wire. The eventual result of this change in the flow profile is that the conductivity increases with increasing e-e scattering rate, the Gurzhi effect. This behavior becomes more pronounced upon decreasing l_{ee}, and the profile becomes similar to the classical, laminar Poiseuille flow. Ultimately, however, the flow is limited by the bulk-impurity scattering, as shown by the curve in Fig. 8 for the smallest value of l_{ee}. The electrons in the middle of the wire have a drift velocity equal to the bulk value, whereas close to the boundaries the drift velocity goes to zero.

In this Section we have demonstrated which flow phenomena may occur in a wire with both diffusive impurity scattering as well as non-resistive e-e scattering. In the next Section we present how the theory can be brought into agreement with the experiments.

V. COMPARISON BETWEEN EXPERIMENT AND THEORY

Now that we have found that both the Knudsen and the Gurzhi effect as observed in the experiments, cf. Sec. II, can at least qualitatively be understood by the theory of the previous Sections, we wish to make a more quantitative comparison. Note, that the experimental traces are dV/dI versus I curves, whereas the theoretical results provide L_{eff} as a function of l_b, l_{ee}, and W.

The resistance R of the sample, as measured in the experiment, is due to two contributions. First, there is the resistance of the wire itself. As shown in Ref. 36, this is equal — to a good approximation — to the sum of the Drude resistance and the Sharvin contact resistance.[37] The second contribution R_0 is due to the unbounded regions in the 2DEG between the Ohmic contacts and the entrance of the wire (see inset to Fig. 1). Note, that in an ideal four-probe measurement, the contacts should be so close to the entrance of the wire, that this contribution would be absent. In our samples, the typical distance between the contacts and the wire is on the order of 200 μm. The actual value of R_0 may vary from wire to wire, and with the lattice temperature. From previous experiments we estimate $R_0 \approx 60 - 90\,\Omega$. We thus have for the resistance[36]

$$R = R_0 + \frac{h\pi}{2e^2 k_F W} + \frac{L}{W\sigma}\,, \tag{29}$$

in which the second term is the Sharvin resistance[37] and the third the Drude resistance. The conductivity σ is given by Eq. (19). The values for L, W, n, and l_b for each wire are displayed in Table I. Due to the electrostatic depletion, the width W of the wires is slightly smaller than the lithographic width of the gate structure. For wire I we take $W = 3.5\,\mu$m and for wires II and III $W = 3.6\,\mu$m.

The theoretical L_{eff} versus l_{ee} curve can now be transformed into an R versus I curve in a three step procedure. First, we apply Eq. (3), which gives the electron temperature T_e against I. Then, l_{ee} is determined as a function of T_e through Eq. (4). Finally, the Boltzmann theory provides L_{eff} (and thus σ) for the given l_{ee}, so that the resistance is given

by Eq. (29). There is a little subtlety here, since the resulting conductivity σ is already used in Eq. (3). One could adopt two approaches: The first would be to neglect the dependence of σ here and simply use its $I = 0$ value in Eq. (3). The second approach, which we have applied, is to find a self-consistent value of σ and l_{ee} in a numerical procedure. Actually, this only slightly changes the I-axis. From the R versus I curve the differential resistance dV/dI versus I is found.[17] It should be mentioned that we do expect some deviations in the I-axis, because of the approximate nature of Eq. (3). Because of the limited validity of Eq. (3) we can only treat the regime $|I| < 20\mu$A. This is sufficient since we only aim to model the Knudsen and the Gurzhi regimes. The dissipative behavior due to the heating of the lattice, which is observed for higher currents in Figs. 2 and 3, is not treated in the comparison.

In Fig. 9 we apply the above analysis for the differential resistance of wire II at $T = 1.8$ K. The experimental curve is a blow-up of the lowest temperature trace in Fig. 3. The theoretical curves are for various boundary-scattering parameters and correspond to the plots in Fig. 7 (since $l_b = 5.5W$). It should be stressed, that R_0 is not included in the theoretical curves, since its precise value is not known. This will be the case for all the comparisons. Clearly the numerical results for a constant specularity coefficient display a far too weak Knudsen and Gurzhi behavior. Both effects can be increased by decreasing p, but this also enhances the $I = 0$ resistance to unreasonable values. The plots in which the boundary scattering is taken to be angle dependent — using Eq. (13) — display a much better resemblance with the experiment. Our experiments thus clearly indicate the validity of Soffer's model[21] for boundary scattering in split-gate defined wires. We find the best agreement with $\alpha = 0.7$. At $I = 0$ the difference between the experimental and the theoretical resistance is 83 Ω, which is within the right range of R_0.

We have applied the same analysis to the $T = 1.5$ K result of wire I. As noted above, the magnitude of the Knudsen effect is much smaller than in wires II and III due to the lower ratio of $l_b/W = 3.5$. This is indeed what is found in the theoretical calculation. The comparison between theory and experiment is given in the inset to Fig. 2. We have found that for wire I $\alpha = 0.6$ yields the best agreement.

The values of α that emerge from the comparisons imply that the root-mean-square boundary roughness of the gate-defined wires $\delta \approx 2.5\,$nm and that approximately 80% of the boundary scattering is specular. This is consistent with earlier magneto-resistance and electron-focusing experiments in gate-defined 2DEG systems.[13,38] Note, that in the potassium-wires used for hydrodynamic electron-flow experiments the boundary scattering is much more diffusive, values of $\alpha \approx 25$ are used.[10]

Finally, we investigate the resistance behavior when the lattice temperature is increased. The experimental curves for wire II and III for T =1.8, 3.5, and 4.5 K are given in Fig. 3. The change in lattice temperature both influences Eq. (3) as well as the bulk mean free path l_b, which also includes some electron-phonon scattering. The difference in the $I = 0$ resistance for the three temperatures are thus caused by changes in l_b and in l_{ee}. Both increase the resistance with increasing lattice temperature. The decrease in l_{ee} causes a part of the Knudsen correction to be already incorporated in the $I = 0$ value of dV/dI. From temperature-dependent mobility measurements we have $l_b = 18.5\,\mu$m at $T = 3.1$ K and $l_b = 17.1\,\mu$m at $T = 4.5$ K. Note, that for the theoretical analysis at $T = 3.1, 4.5$ K we push Eq. (3) slightly beyond its range of validity. A comparison with theory for $\alpha = 0.7$ is

presented in Fig. 3. For both wire II and wire III, the theoretical curves are quite similar to the experiments as to shape and amplitude. The decrease in the Knudsen effect with increasing lattice temperature is indeed found. We do observe, however, a difference with the experiment for the additional offset between the individual curves. This is probably caused by a temperature dependence in R_0.

VI. DISCUSSION AND CONCLUSIONS

Our experiments have provided an unambiguous demonstration of the occurrence of Knudsen and Gurzhi flow regimes in electron transport. The existence of these transport regimes has already been anticipated in the 1960's.[2,5] Although some aspects of hydrodynamic electron flow have been observed in potassium wires,[7–9] it is the high-mobility obtained in (Al,Ga)As heterostructures in combination with nano-lithography techniques that has made the observation of the complete transition from the Knudsen to the Gurzhi flow regime accessible. The current-heating technique appears to be an essential tool, by which the e-e scattering rate can be varied, while keeping the other types of scattering unaltered. Due to the point-contact thermometry we are able to determine the electron temperature inside the wire as a function of the current. Although hydrodynamic electron flow has been predicted many years ago, its actual observation in our devices and the sheer size of the effects is quite astonishing.

We have developed a theory based on the Boltzmann transport equation. The theory is more complex than that for gas-flow because of the presence of bulk-impurity scattering. Most previous theoretical work[5,10,11,23] is only applicable to certain limiting flow regimes. Our approach is more general, in the sense that it provides the conductivity for the complete flow regime, i.e. for any value of the wire width, the e-e scattering length, and the bulk-impurity mean free path. It should be mentioned that we have made two essential simplifications in our Boltzmann approach. First, we assume isotropic impurity scattering instead of the small-angle scattering known to occur in a 2DEG. Second, we apply a simple e-e scattering term due to Callaway,[26] which only takes into account the conservation of the total momentum. At this moment, we do not see a method of solution of the Boltzmann equation with on the one hand more realistic scattering terms, and which is on the other hand applicable to the complete transport regime. However, our method already shows how complex the flow behavior becomes due to the combination of resistive impurity scattering as well as partly diffusive boundary scattering and non-resistive e-e scattering.

A quantitative comparison between experiment and the Boltzmann theory can be made, since the electron temperature and thus the e-e scattering length inside the wire can be inferred from experiment. The obtained agreement is quite good. This proves that in spite of its simplifications our Boltzmann theory contains the essential physical ingredients to describe the experiments. Our results show that the Soffer model[21] for angle-dependent boundary scattering is more appropriate to describe the scattering with the gate-defined wire boundaries than a constant specularity coefficient. Apart from the determination of the specularity parameter, our comparison is only based on experimental data and contains no fitting.

It would be of interest to perform further experiments on hydrodynamic electron flow. Promising areas of investigation are the influence of more diffusive boundary scattering, e.g.

in wires defined by reactive ion etching or ion exposure, and the application of a magnetic field. The theoretical analysis given here can be adopted in a straightforward manner to describe the transition from Knudsen to Gurzhi flow in three-dimensional systems.

ACKNOWLEDGMENTS

We thank G. E. W. Bauer, C. W. J. Beenakker, and H. van Houten for valuable discussions, and E. E. Bende, O. J. A. Buyk, M. Kemerink, and M. A. A. Mabesoone for technical assistance. The heterostructures were grown by C. T. Foxon, presently at the University of Nottingham, UK. L. W. M. acknowledges the kind hospitality of Y. Aoyagi, K. Ishibashi, J. Kusano, and S. Namba during a visit to the Laboratory for Quantum Materials, RIKEN, Saitama, Japan, where this research was initiated. M. J. M. de J. was supported by the "Nederlandse organisatie voor Wetenschappelijk Onderzoek" (NWO) and by the "Stichting voor Fundamenteel Onderzoek der Materie" (FOM).

APPENDIX A:

We show how Eq. (16) can be derived. The combination of the Boltzmann equation (7) with the impurity (9) and the e-e (11) scattering terms yields

$$\begin{aligned} &-eEv_F\cos\varphi + v_F\sin\varphi\,\frac{\partial\chi(y,\varphi)}{\partial y} = \\ &-\frac{\chi(y,\varphi)}{\tau} + \frac{1}{\tau}\int_0^{2\pi}\frac{d\varphi'}{2\pi}\chi(y,\varphi') \\ &+\frac{1}{\tau_{ee}}\int_0^{2\pi}\frac{d\varphi'}{\pi}\cos(\varphi-\varphi')\chi(y,\varphi')\,, \end{aligned} \tag{A1}$$

with $\tau^{-1} = \tau_b^{-1} + \tau_{ee}^{-1}$ For the time-independent case the drift velocity has no component in the y-direction

$$\int_0^{2\pi}\frac{d\varphi}{\pi}\sin\varphi\,\chi(y,\varphi) = 0\,. \tag{A2}$$

As a result the $\cos(\varphi-\varphi')$ in the last term in Eq. (A1) can be replaced by $\cos\varphi\cos\varphi'$. Substitution of the parametrization (15) yields

$$\begin{aligned} &-\cos\varphi + \cos\varphi\,\sin\varphi\,\frac{\partial l_{\rm eff}(y,\varphi)}{\partial y} = \\ &-\frac{\cos\varphi\, l_{\rm eff}(y,\varphi)}{l} + \frac{1}{l}\int_0^{2\pi}\frac{d\varphi'}{2\pi}\cos\varphi'\, l_{\rm eff}(y,\varphi') \\ &+\frac{\cos\varphi}{l_{ee}}\int_0^{2\pi}\frac{d\varphi'}{\pi}\cos^2\varphi'\, l_{\rm eff}(y,\varphi')\,. \end{aligned} \tag{A3}$$

Analysis of Eq. (A3) shows that $l_{\rm eff}(y,\varphi)$ and $l_{\rm eff}(y,\pi-\varphi)$ obey precisely the same equation. In addition the boundary conditions (14) are equal. Due to this symmetry we have

$$l_{\rm eff}(y,\varphi) = l_{\rm eff}(y,\pi-\varphi)\,. \tag{A4}$$

In combination with Eq. (15) it follows that the non-equilibrium density is zero for all y

$$\int\limits_0^{2\pi} d\varphi\,\chi(y,\varphi) = eE\int\limits_0^{2\pi} d\varphi\,\cos\varphi\, l_{\rm eff}(y,\varphi) = 0\,. \tag{A5}$$

Thus, the second term on the r. h. s. of Eq. (A3) vanishes. [This equally applies to the second terms on the r. h. s. of Eqs. (9), (11), and (14).] As a result Eq. (A3) leads to the integro-differential equation (16) of the main text.

APPENDIX B:

In this Appendix it is shown how some results presented in Sec. IV can be obtained. We study the conductivity and its first order correction due to e-e scattering for a wire with diffusive boundary scattering ($p=0$). By multiplication of Eq. (21) with $\cos^2\varphi$ and integration over φ one finds

$$\begin{aligned}\tilde{l}_{\rm eff}(y) = l - \frac{2l}{\pi}\int\limits_0^{\pi/2} d\varphi\,\cos^2\varphi\,\left[e^{-y/l\sin\varphi} + e^{-(W-y)/l\sin\varphi}\right] \\ + \frac{2}{\pi l_{ee}}\int\limits_0^{W} dy'\int\limits_0^{\pi/2} d\varphi\,\frac{\cos^2\varphi}{\sin\varphi}\,e^{-|y-y'|/l\sin\varphi}\tilde{l}_{\rm eff}(y')\,.\end{aligned} \tag{B1}$$

In the limit of very small e-e scattering rate ($l_{ee}\gg l_b, W$) the next step is to solve Eq. (B1) perturbatively. The first two terms of Eq. (B1) are substituted into the third term. An additional integration over y then yields the conductivity [cf. Eq. (19)]

$$\begin{aligned}L_{\rm eff} = l - \frac{4l^2}{\pi W}I(l/W) + \frac{l^2}{l_{ee}} - \frac{8l^3}{\pi l_{ee}W}I(l/W) \\ + \frac{8l^3}{\pi^2 l_{ee}W}K(l/W)\,,\end{aligned} \tag{B2}$$

$$I(\lambda) = \int\limits_0^1 du\,u\sqrt{1-u^2}\left(1-e^{-1/\lambda u}\right)\,, \tag{B3}$$

$$\begin{aligned}K(\lambda) = \int\limits_0^1 du\,u\sqrt{1-u^2}\int\limits_0^1 dv\,v\sqrt{1-v^2} \\ \times\left[\frac{1-e^{-1/\lambda u-1/\lambda v}}{u+v} + \frac{e^{-1/\lambda u}-e^{-1/\lambda v}}{u-v}\right]\,.\end{aligned} \tag{B4}$$

In the absence of e-e scattering ($l_{ee} = \infty$) the conductivity is given by[13]

$$L_{\text{eff}} = l_b - \frac{4l_b^2}{\pi W} I(l_b/W) \,. \tag{B5}$$

The first order correction due to e-e scattering can be found by substracting Eq. (B5) from (B2) and expanding $l = l_b - l_b^2/l_{ee}$. The result can be evaluated analytically in two limits. For a very wide wire $l_b \ll W$ we use the results

$$\lim_{\lambda\to 0} I(\lambda) = \frac{1}{3} \,, \tag{B6a}$$

$$\lim_{\lambda\to 0} K(\lambda) = \frac{\pi}{30} \,, \tag{B6b}$$

which provide Eqs. (24) and (25). In the opposite limiting regime of a very narrow wire ($l_b \gg W$) the integrals (B3) and (B4) are more complex. We have obtained the following series expansions

$$\lim_{\lambda\to\infty} I(\lambda) = \frac{\pi}{4\lambda} - \frac{1}{2\lambda^2}(\ln 2\lambda + \tfrac{1}{2} - \gamma) + \mathcal{O}(\lambda^{-3}) \,, \tag{B7a}$$

$$\lim_{\lambda\to\infty} K(\lambda) = \frac{\pi^2}{8\lambda} - \frac{\pi}{2\lambda^2}(\ln 2\lambda + \tfrac{1}{2} - \gamma) + \mathcal{O}(\lambda^{-3}) \,, \tag{B7b}$$

where $\gamma \simeq 0.577$ is Euler's constant. These results yield Eqs. (22) and (23).

The first order correction due to e-e scattering in between these two regimes can be evaluated by substracting Eq. (B5) from (B2). We then have

$$\Delta L_{\text{eff}} = \frac{l_b}{l_{ee}} \left[\frac{8l_b^2}{\pi^2 W} K(l_b/W) - \frac{4l_b}{\pi} J(l_b/W) \right] \,, \tag{B8}$$

$$J(\lambda) = \int_0^1 du \sqrt{1-u^2}\, e^{-1/\lambda u} \,. \tag{B9}$$

By numerical integration of I, J, and K the plots in Fig. 4 are obtained.

REFERENCES

* Also at: Instituut-Lorentz, University of Leiden, 2300 RA Leiden, The Netherlands.

† Present and permanent address: 2. Physikalisches Institut, RWTH Aachen, D-52056 Aachen, Germany.

[1] M. Knudsen, Ann. Phys. **28**, 75 (1909).

[2] J. M. Ziman, *Electrons and Phonons*, (Oxford Univ. Press, Oxford, England, 1960).

[3] In this paper electron-electron (e-e) scattering only refers to *momentum-conserving* scattering. These processes are also known as *normal* electron-electron scattering. In contrast, *umklapp* electron-electron scattering does not conserve momentum, and is explicitly denoted each time it is mentioned in the text. As we argue in the main text *umklapp* electron-electron scattering is absent in the two-dimensional electron gas, which is studied in this paper.

[4] M. Kaveh and N. Wiser, Adv. Phys. **33**, 257 (1984).

[5] R. N. Gurzhi, Zh. Eksp. Teor. Fiz. **44**, 771 (1963) [Sov. Phys. JETP **17**, 521 (1963)]; Zh. Eksp. Teor. Fiz. **46**, 719 (1964) [Sov. Phys. JETP **19**, 490 (1964)]; Usp. Fiz. Nauk. **94**, 689 (1968) [Sov. Phys. Usp. **11**, 255 (1968)].

[6] J. Bass, W. P. Pratt, Jr., and P. A. Schroeder, Rev. Mod. Phys. **62**, 645 (1990).

[7] Z.-Z. Yu, M. Haerle, J. W. Zwart, J. Bass, W. P. Pratt, Jr., and P. A. Schroeder, Phys. Rev. Lett. **52**, 368 (1984).

[8] J. Zhao, W. P. Pratt, Jr., H. Sato, P. A. Schroeder, and J. Bass, Phys. Rev. B **37**, 8738 (1988).

[9] Z.-Z. Yu, S. Yin, M. L. Haerle, Y. J. Qian, H. Bidadi, W. P. Pratt, Jr., P. A. Schroeder, and J. Bass, Phys. Rev. B **40**, 7601 (1989).

[10] D. Movshovitz and N. Wiser, J. Phys.: Condens. Matter **2**, 8053 (1990).

[11] D. Movshovitz and N. Wiser, Phys. Rev. B **41**, 10503 (1990).

[12] Y.-J. Qian, W. P. Pratt, Jr., P. A. Schroeder, D. Movshovitz, and N. Wiser, J. Phys.: Condens. Matter **3**, 9459 (1991).

[13] C. W. J. Beenakker and H. van Houten, Solid State Phys. **44**, 1 (1991).

[14] B. L. Gallagher, T. Galloway, P. Beton, J. P. Oxley, S. P. Beaumont, S. Thoms, and C. D. W. Wilkinson, Phys. Rev. Lett. **64**, 2058 (1990).

[15] L. W. Molenkamp, H. van Houten, C. W. J. Beenakker, R. Eppenga, and C. T. Foxon, Phys. Rev. Lett. **65**, 1052 (1990).

[16] L. W. Molenkamp, Th. Gravier, H. van Houten, O. J. A. Buyk, M. A. A. Mabesoone, and C. T. Foxon, Phys. Rev. Lett. **68**, 3765 (1992).

[17] The relation between the resistance and the differential resistance at a current I is: $dV/dI = R + IdR/dI$.

[18] K. Fuchs, Proc. Cambridge Philos. Soc. **34**, 100 (1938).

[19] R. B. Dingle, Proc. R. Soc. London Ser. A **201**, 545 (1950).

[20] R. G. Chambers, Proc. R. Soc. London Ser. A **202**, 378 (1950).

[21] S. B. Soffer, J. Appl. Phys. **38**, 1710 (1967).

[22] J. R. Sambles, K. C. Elsom, and T. W. Preist, J. Phys. F **12**, 1169 (1982).

[23] R. N. Gurzhi, A. N. Kalinenko, and A. I. Kopeliovich, Zh. Eksp. Teor. Fiz. **96**, 1522 (1989) [Sov. Phys. JETP **69**, 863 (1989)].

[24] J. E. Black, Phys. Rev. B **21**, 3279 (1980).

[25] S. De Gennaro and A. Rettori, J. Phys. F **14**, L237 (1984); **15**, 2177 (1985).

[26] J. Callaway, Phys. Rev. **113**, 1046 (1959).
[27] A. V. Chaplik, Zh. Eksp. Teor. Fiz. **60**, 1845 (1971) [Sov. Phys. JETP **33**, 997 (1971)].
[28] G. F. Giuliani and J. J. Quinn, Phys. Rev. B **26**, 4421 (1982).
[29] B. Laikhtman, Phys. Rev. B **45**, 1259 (1992).
[30] R. N. Gurzhi, A. N. Kalinenko, and A. I. Kopeliovich, Phys. Low-Dim. Struct. **2**, 75 (1994).
[31] L. W. Molenkamp and M. J. M. de Jong, Phys. Rev. B **49**, 5038 (1994).
[32] P. Streda, J. Phys. Condens. Matter **1**, 1025 (1989).
[33] T. Kawamura and S. Das Sarma, Phys. Rev. B **45**, 3612 (1992).
[34] A. Yacoby, U. Sivan, C. P. Umbach, and J. M. Hong, Phys. Rev. Lett. **66**, 1938 (1991).
[35] L. W. Molenkamp, M. J. P. Brugmans, H. van Houten, and C. T. Foxon, Semicond. Sci. Technol. **7**, B228 (1992).
[36] M. J. M. de Jong, Phys. Rev. B **49**, 7778 (1994).
[37] Yu. V. Sharvin, Zh. Eksp. Teor. Fiz. **48**, 984 (1965) [Sov. Phys. JETP **21**, 655 (1965)].
[38] T. J. Thornton, M. L. Roukes, A. Scherer, and B. P. Van der Gaag, Phys. Rev. Lett. **63**, 2128 (1989).

FIGURES

FIG. 1. Dependence of the thermovoltage $V_{\rm trans} \equiv V_6 - V_3$ and of the difference between the electron and the lattice temperature $T_e - T$ on the heating current I measured for wire I at $T = 1.5$ K. Point contact AB is adjusted for maximum, CD for zero thermopower. Inset: Schematical layout of the gates (hatched areas) used to define a wire with point-contact voltage probes. The wire width W is typically 4 μm, the length L varies between 20 and 120 μm. The crossed boxes denote ohmic contacts. The coordinates used for the theory are indicated.

FIG. 2. Differential resistance dV/dI of wire I as a function of current I for lattice temperatures $T = 24.7$, 20.4, 17.3, 13.6, 10.4, 8.7, 4.4, and 1.5 K (from top to bottom). The upper panel (a) of the inset is a magnification of the T =1.5 K result. The lower panel (b) displays the result of the theory described in Sec. V.

FIG. 3. Differential resistance dV/dI vs. current I for wire II and III for lattice temperatures of (from top to bottom) T =4.5, 3.1, and 1.8 K. At higher current levels, dV/dI exhibits a quasi-quadratic increase with current, similar to that in Fig. 2. Left panel (IIa) and (IIIa): experimental traces; right panel (IIb) and (IIIb): results of calculations, see Sec. V.

FIG. 4. The conductivity $L_{\rm eff}$ in the absence of e-e scattering and the first order correction $\Delta L_{\rm eff}$ due to e-e scattering against the bulk-impurity mean free path l_b. Results are for a two-dimensional wire with diffusive boundary scattering ($p = 0$) according to Eqs. (B5) and (B8), respectively.

FIG. 5. The conductivity $L_{\rm eff}$ of a wire with diffusive boundary scattering ($p = 0$) against the e-e scattering mean free path l_{ee} for various bulk-impurity mean free paths l_b.

FIG. 6. The conductivity $L_{\rm eff}$ of a wire with a mean free path $l_b = 5W$ against the e-e scattering mean free path l_{ee} for various specularity coefficients p. The inset shows the relative change in the conductivity at the Knudsen maximum (which corresponds to the *minimum* in the conductivity).

FIG. 7. Comparison of the conductivity $L_{\rm eff}$ as a function of l_{ee} for constant boundary-scattering coefficients (dotted curves) and for angle-dependent coefficients (solid lines) according to Eq. (13). To have approximately equal conductivity in the absence of e-e scattering the comparison is between (top to bottom) $p = 0.895, 0.87, 0.845$ and $\alpha = 0.6, 0.7, 0.8$, respectively. The bulk-impurity mean free path $l_b = 5.5W$.

FIG. 8. Velocity profiles inside the wire show how the flow changes from the Knudsen upto the Gurzhi regime. Depicted are the (normalized) drift velocity $\tilde{l}_{\rm eff}(y)$ as a function of the transverse coordinate y for $l_{ee}/W = 100$ ($\times$), 1 ($\triangle$), 0.1 ($+$), 0.01 ($\square$), and 0.001 ($\diamond$). The inset shows the conductivity $L_{\rm eff}$ as a function of the e-e scattering length l_{ee} and the symbols that indicate to which value each flow profile corresponds. Results are for the bulk mean free path $l_b = 5.5W$ and for angle-dependent boundary scattering with $\alpha = 0.7$.

FIG. 9. Differential resistance dV/dI versus current I for wire II. The top curve is the experimental result at $T = 1.8$ K, as shown for a larger current range in Fig. 3. The other curves are theoretical results for various boundary-scattering parameters. The dotted lines are calculated with a constant specularity coefficient $p = 0.845, 0.87, 0.895$ (top to bottom). The solid lines are calculated for angle-dependent boundary scattering, with $\alpha = 0.8, 0.7, 0.6$ (top to bottom). Best agreement with experiment is found for $\alpha = 0.7$ (thick curve).

TABLES

TABLE I. Length L, lithographic width $W_{\rm lith}$, electrical width W, electron density n, mean free path $l_{\rm b}$ [at 1.5 K (sample I) and 1.8 K (sample II & III)], and specularity parameter α of the samples discussed in this paper.

Sample	L (μm)	$W_{\rm lith}$ (μm)	W (μm)	n (10^{11}cm^{-2})	l_b (μm)	α
I	20.2	3.9	3.5	2.2	12.4	0.6
II	63.7	4.0	3.6	2.7	19.7	0.7
III	127.3	4.0	3.6	2.7	19.7	0.7

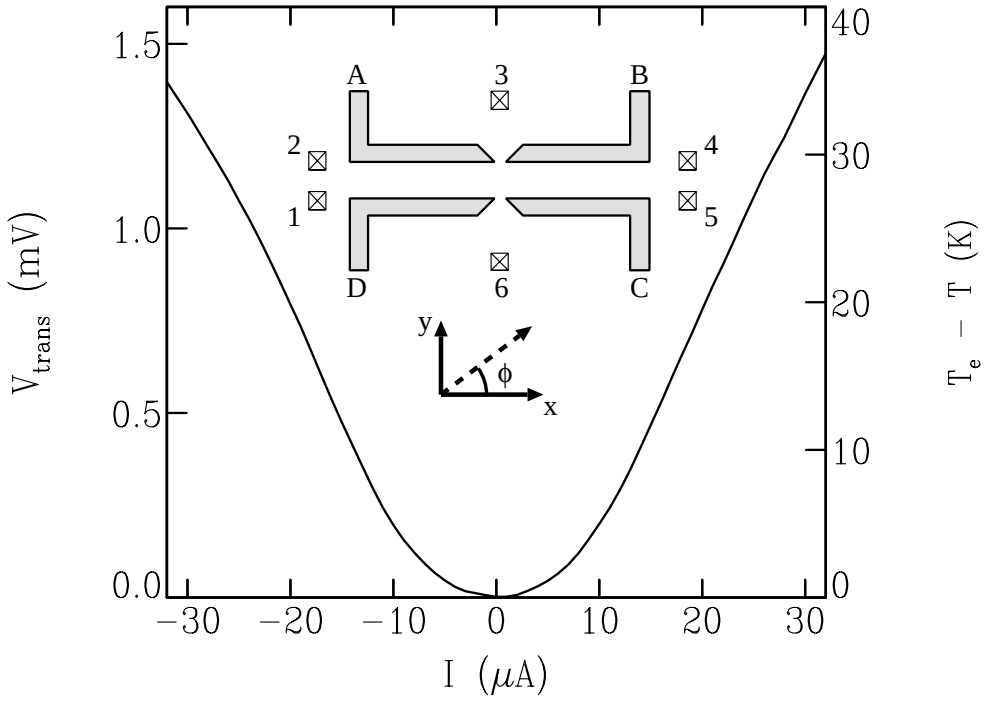

Fig. 1

M. J. M. de Jong and L. W. Molenkamp
Hydrodynamic electron flow in high-mobility wires

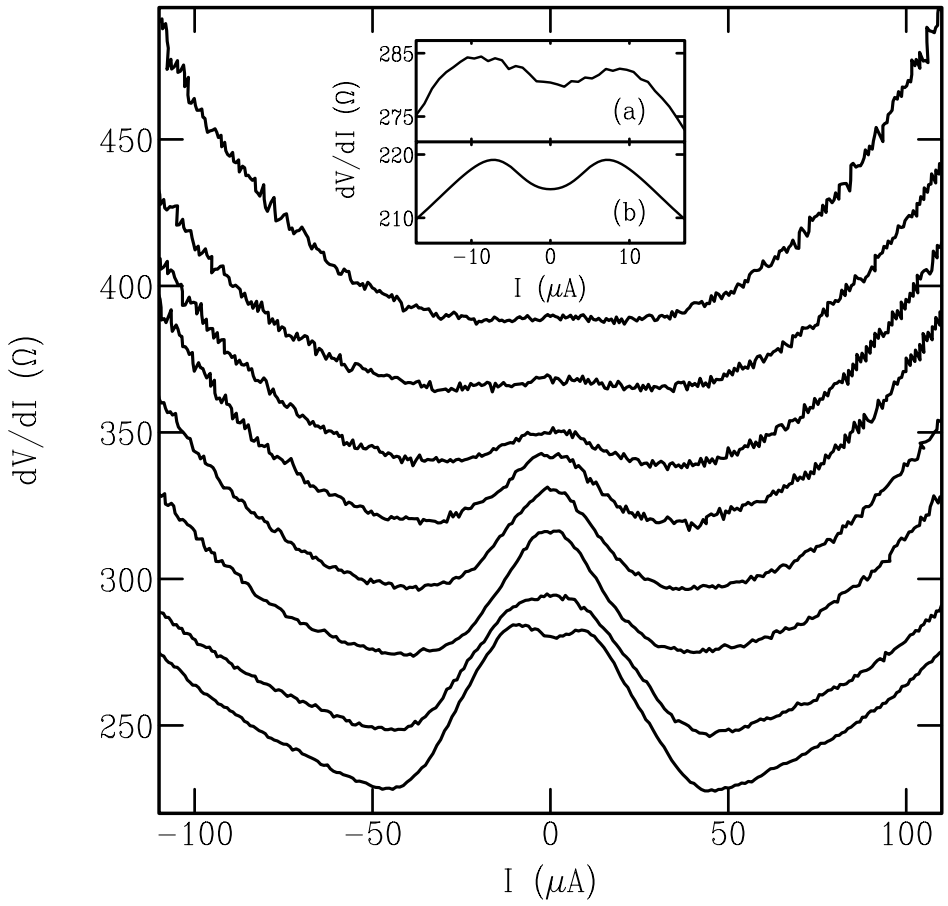

Fig. 2

M. J. M. de Jong and L. W. Molenkamp
Hydrodynamic electron flow in high-mobility wires

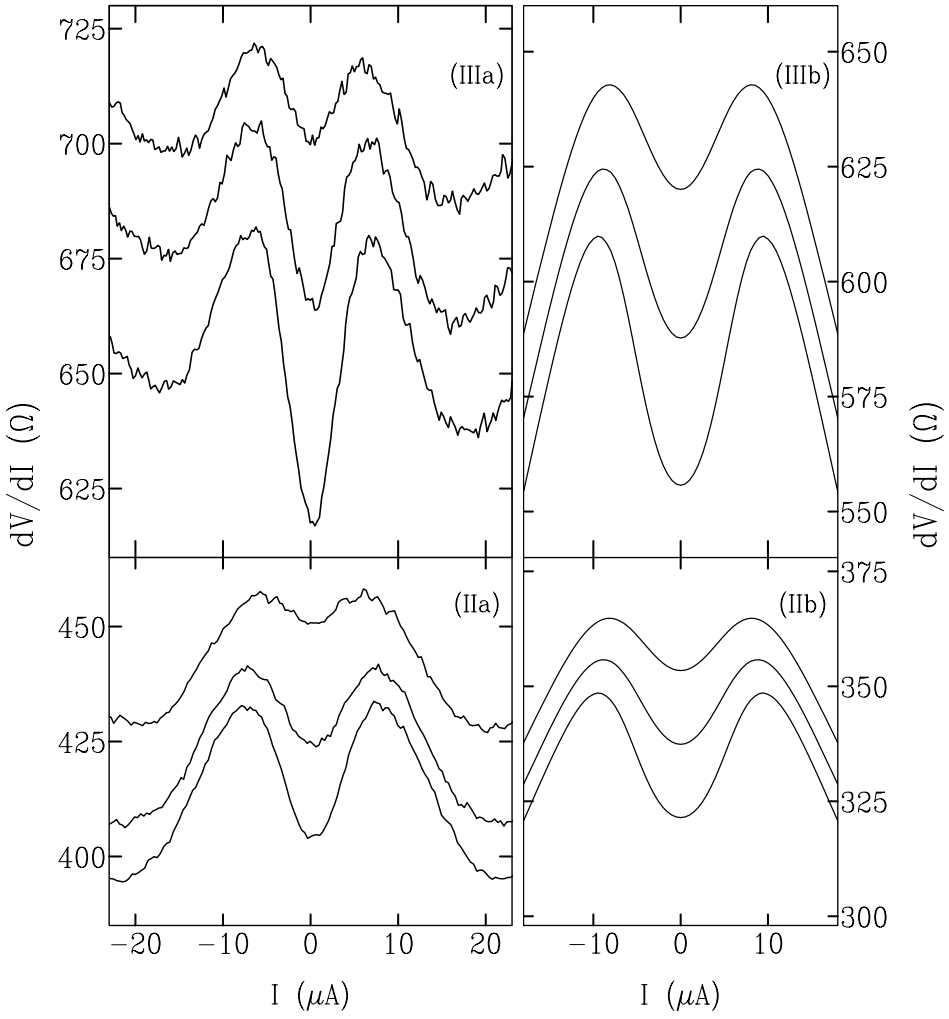

Fig. 3

M. J. M. de Jong and L. W. Molenkamp
Hydrodynamic electron flow in high-mobility wires

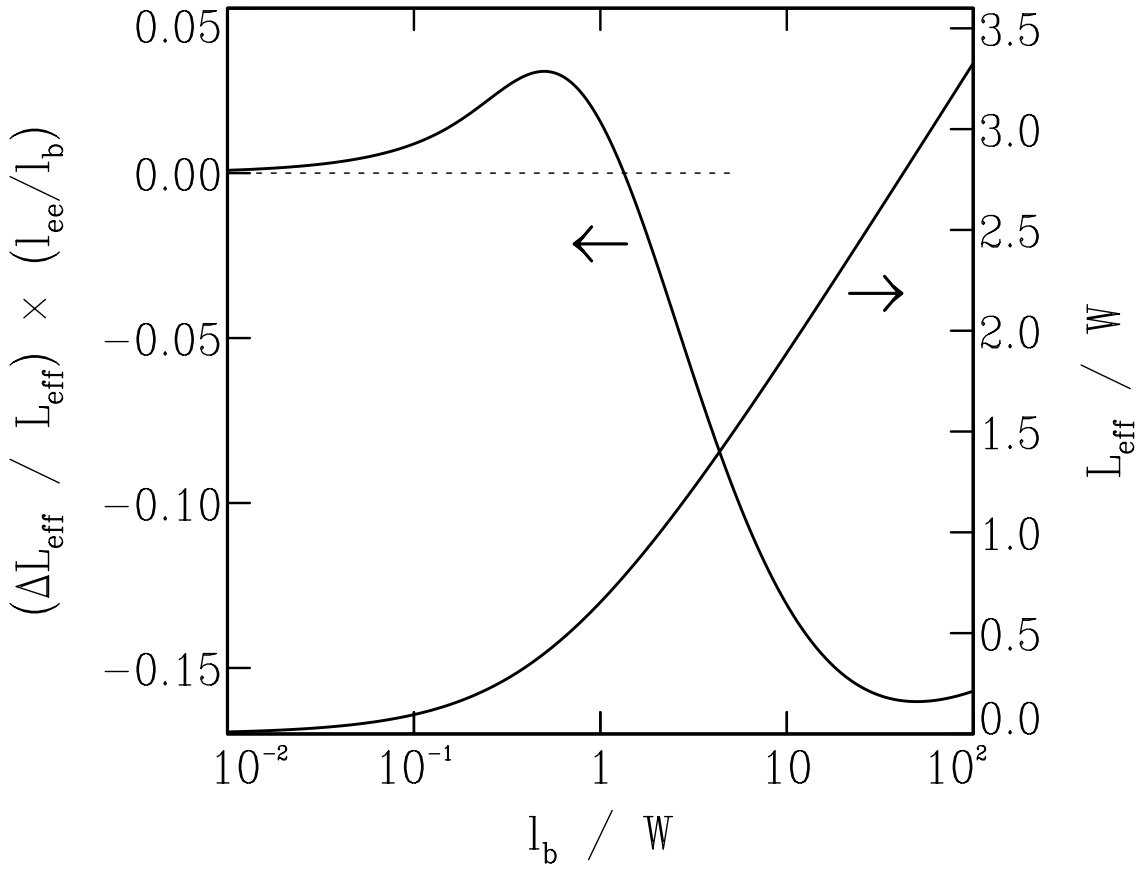

Fig. 4

M. J. M. de Jong and L. W. Molenkamp
Hydrodynamic electron flow in high-mobility wires

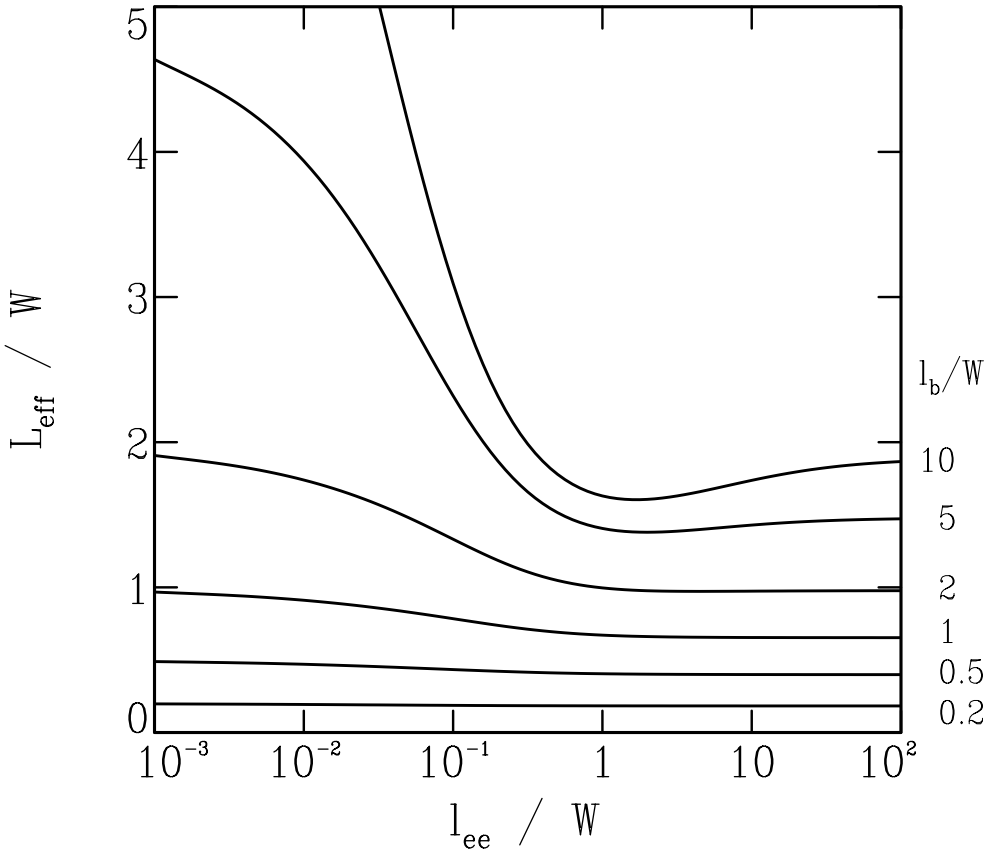

Fig. 5

M. J. M. de Jong and L. W. Molenkamp
Hydrodynamic electron flow in high-mobility wires

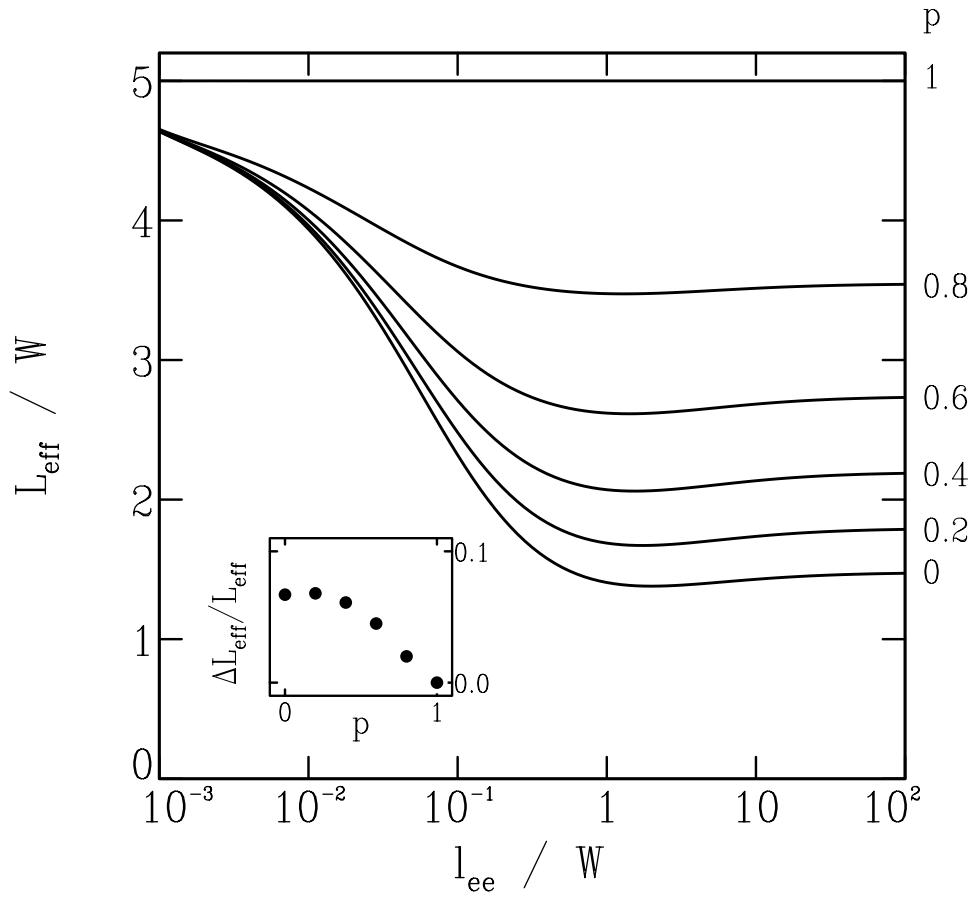

Fig. 6

M. J. M. de Jong and L. W. Molenkamp
Hydrodynamic electron flow in high-mobility wires

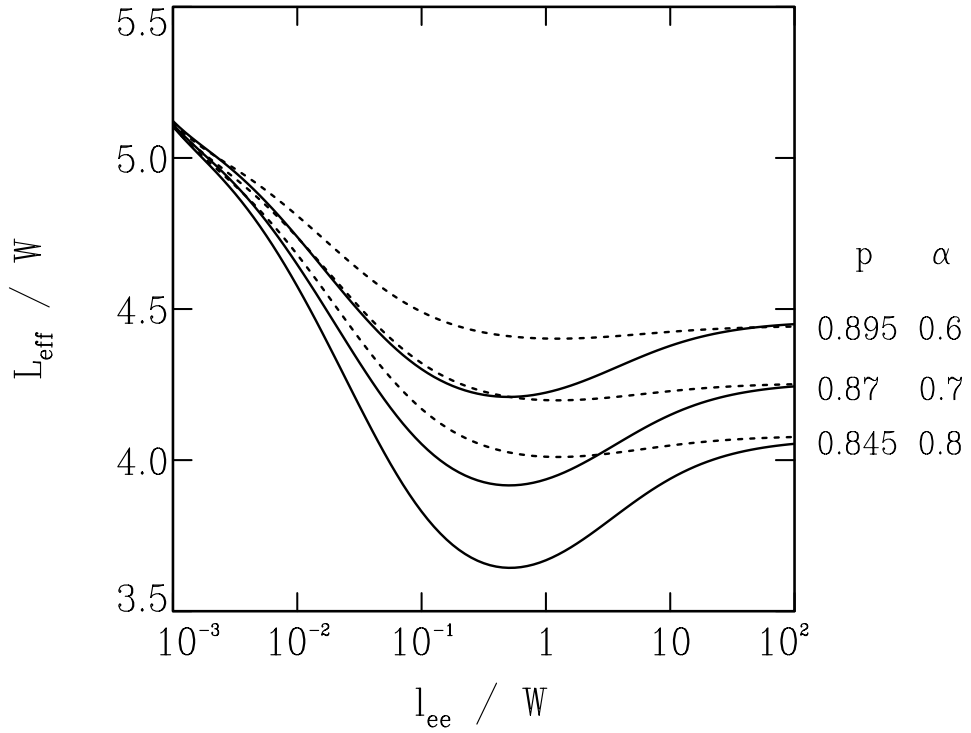

Fig. 7

M. J. M. de Jong and L. W. Molenkamp
Hydrodynamic electron flow in high-mobility wires

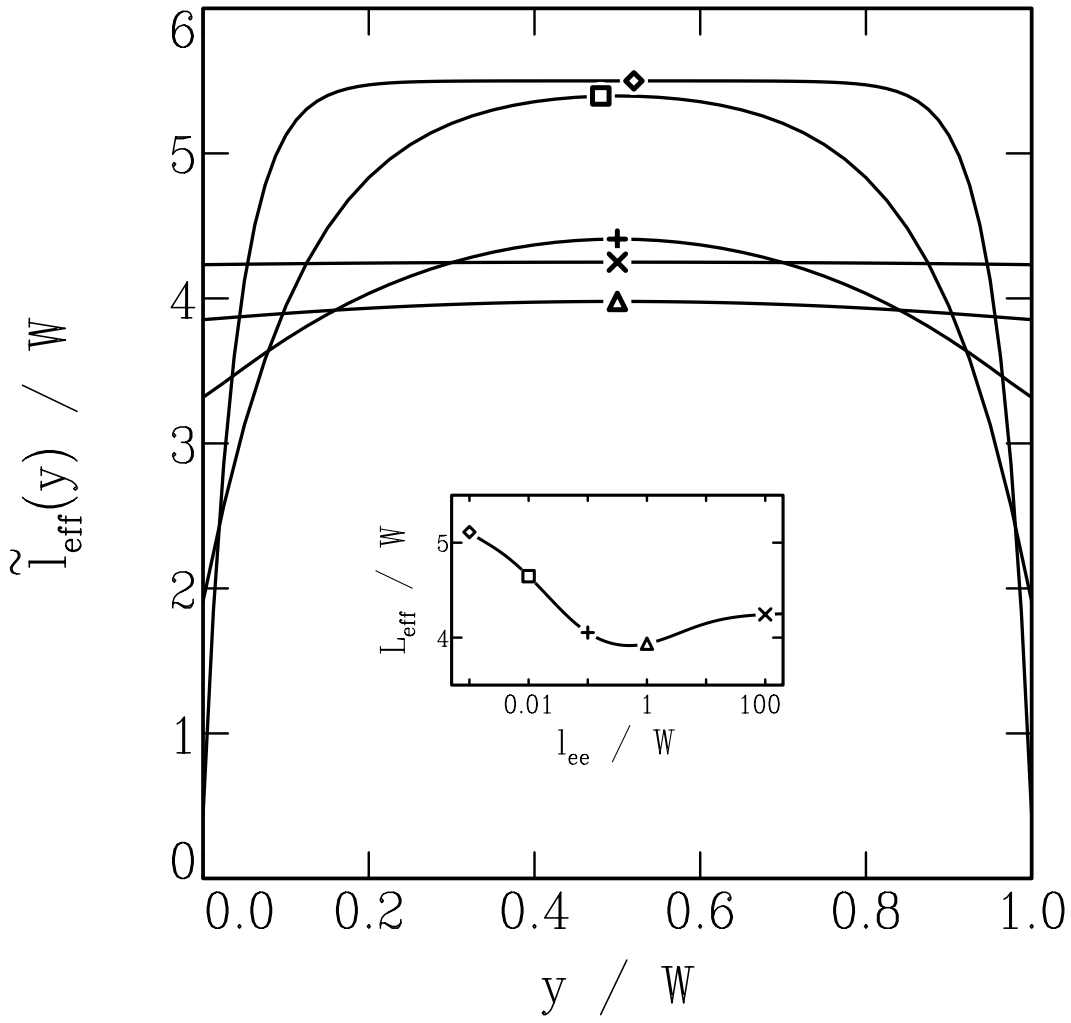

Fig. 8

M. J. M. de Jong and L. W. Molenkamp
Hydrodynamic electron flow in high-mobility wires

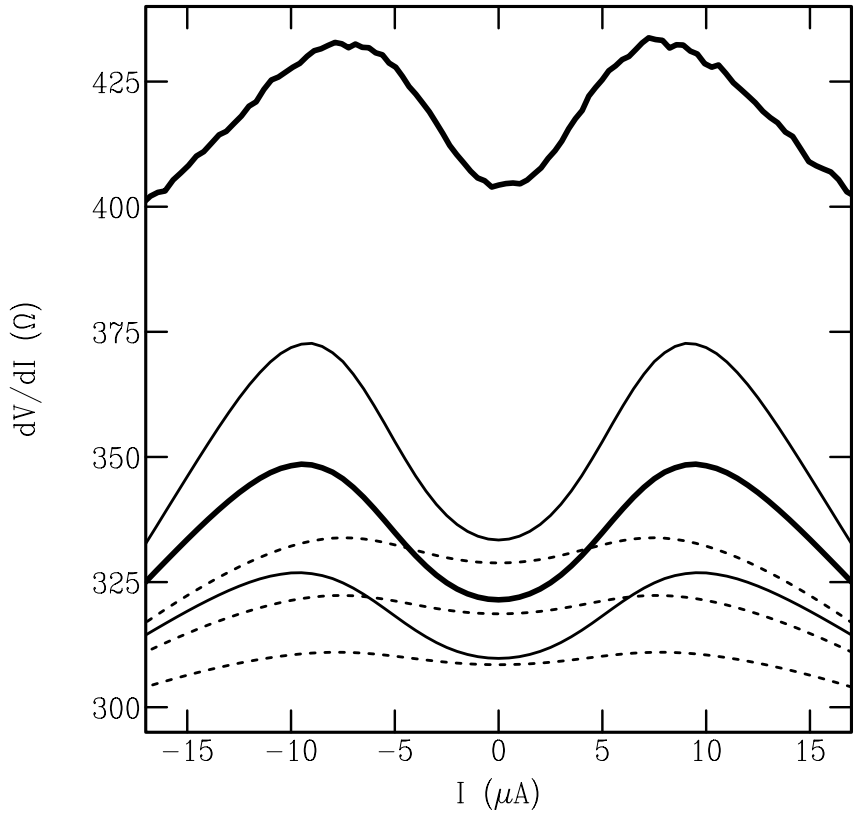

Fig. 9

M. J. M. de Jong and L. W. Molenkamp
Hydrodynamic electron flow in high-mobility wires